9-1-2001

The first detection of coherent emission from radio pulsars

F. A. Jenet

S. B. Anderson

T. A. Prince

Recommended Citation

F. A. Jenet, et. al., (2001) The first detection of coherent emission from radio pulsars.Astrophysical Journal558:1302. DOI: http://doi.org/10.1086/322469

THE ASTROPHYSICAL JOURNAL, 558:302–308, 2001 September 1

THE FIRST DETECTION OF COHERENT EMISSION FROM RADIO PULSARS

F. A. JENET
Schlumberger-Doll Research Laboratory, Old Quarry Road, Ridgefield, CT 06877; jenet@ridgefield.sdr.slb.com
S. B. ANDERSON
Department of Astronomy, MS 18-34, California Institute of Technology, Pasadena, CA 91125; sba@srl.caltech.edu
AND
T. A. PRINCE
Space Radiation Laboratory, California Institute of Technology, Pasadena, CA 91125; prince@srl.caltech.edu
Received 2000 August 2; accepted 2001 May 7

ABSTRACT

The statistical properties of the radio emission from the pulsars B0823+26, B0950+08, B1133+16, and B1937+21 are studied using high time resolution observations taken at the Arecibo Observatory in Puerto Rico. Temporally coherent non-Gaussian emission has been detected in three of the four observed objects. This is the first time such a phenomenon has been observed. The results have been interpreted using a generalized shot noise model, and various basic physical quantities pertaining to the magnetospheric plasma have been estimated.

Subject headings: pulsars: general — pulsars: individual (B0823+26, B0950+08, B1133+16, B1937+21) — stars: neutron

1. INTRODUCTION

The basic physical processes responsible for pulsar radio-frequency emission have eluded researchers since the discovery of pulsars in the late 1960s. The crux of the problem lies in the high observed brightness temperature ($T \approx 10^{25}$ K). Such temperatures rule out well-understood thermal plasma phenomena, and imply more complicated, barely understood, "coherent" plasma processes (Melrose 1992). Along with this, pulsars exhibit a wide range of phenomenology, including intensity fluctuations on several distinct temporal scales. Timescales of the order of several minutes and greater are attributed to interstellar propagation effects (Rickett 1998; Cordes & Rickett 1998), while shorter timescales are attributed to effects local to the pulsar (Hankins 1996). Hence, a characterization of the radiation field statistics on short timescales has the potential to reveal information about the local environment (i.e., the pulsar magnetosphere), as well as the basic emission process itself. To date, observations have shown that the radiation field can be expressed as an amplitude-modulated Gaussian-noise process. All temporal fluctuations are due to the amplitude modulation. Unfortunately, such a model does little to constrain the basic plasma process responsible for the radio emission. Therefore, it is important to determine the validity of this model. If this model is invalidated, and coherent non-Gaussian statistics are established, theoretical models can no longer rely on the central limit theorem to average away the collective effects of the basic plasma-emission processes. Hence, the results presented in this paper provide strong constraints on the emission process, and require the development of detailed theoretical models, which may need to include both generation and propagation of the intense radiation field in order to fully understand the observations.

In an attempt to juxtapose coherent plasma emission with the previously observed amplitude-modulated Gaussian-noise statistics, researchers have developed the concept of a "fundamental emitter" (Gil 1985; Cordes 1976). A fundamental emitter is an individual coherent emission event. The observed radiation field is an incoherent sum of a large number of these fundamental emission events. If these fundamental emitters exist, then information about the average emitter timescale, the rate of occurrence, and the average emitter intensity is contained within the ensemble-averaged statistics of the received radiation field. Models of the radiation field based on the fundamental emitter concept are called shot noise models. Simple shot noise models are investigated below and are used to interpret the observations.

In the next section, the observations are described along with the various preprocessing steps needed to prepare the data for further analysis. The techniques used to search for coherent non-Gaussian statistics are described in § 3. In § 4, the results of this analysis are presented for pulsars B0823+26, B0950+08, B1133+16, and B1937+21. These results are interpreted in the framework of a generalized shot noise model, and various fundamental parameters are measured in § 5. Lastly, this work is summarized in § 6.

2. OBSERVATIONS AND PREPROCESSING

The data were taken at the 305 m Arecibo radio telescope, using the 430 MHz line feed receiver. Both circular polarizations were 2-bit complex sampled at a rate of 10 MHz ($\Delta t = 100$ ns), and recorded to tape using the recently installed Caltech Baseband Recorder (CBR). Further processing of the data was performed at the Caltech Center for Advanced Computation and Research (CACR), using a 256 processor Hewlett-Packard Exemplar.

The 2-bit complex samples were unpacked and assigned optimum values in order to minimize signal distortion (Jenet & Anderson 1998). The dual-polarization voltage data were corrected for receiver cross-talk using an empirically derived calibration matrix (Stineberg 1982). The effects of the Earth's motion around the Sun were removed by resampling the complex voltage data at a rate necessary to transform the data into the barycentric frame. This rate was calculated using the software package TEMPO (Taylor & Weisberg 1989). The effects of interstellar dispersion were

TABLE 1

ASTROMETRIC AND SPIN PARAMETERS FOR OBSERVED PULSARS

Parameter	B0823+26	B0950+08	B1133+16	B1937+21
R.A. (J2000)	8 26 51.31	9 53 09.316	11 36 03.296	19 39 38.560210
Decl. (J2000)	26 37 25.57	7 55 35.60	15 51 00.69	21 34 08.14166
Distance (kpc)	0.38	0.13	0.27	3.58
Period, $\mathscr{P}$ (ms)	530.65995906	253.06506819	1187.91153608	1.557806468819794
Period derivative $\dot{\mathscr{P}}$ (10^{-15})	1.7236	0.22915	3.73273	10.51193×10^{-5}
Epoch of period and position (MJD)	42716.5	41500.5	41664.5	47500.00
Dispersion measure (cm^{-3} pc)	19.463	2.969	4.847	71.0249

NOTE.—Units of right ascension are hours, minutes, and seconds, and units of declination are degrees, arcminutes, and arcseconds.

removed by coherently dedispersing the data (Jenet et al. 1997; Hankins & Rickett 1975). The dispersion measures used for each source are given in Table 1.

3. ANALYSIS TECHNIQUES

In this section, the statistical techniques used to detect coherent non-Gaussian statistics are described.

3.1. *Ensemble Averaging*

This is a standard technique that is normally used to create average intensity profiles, and is sometimes referred to as "pulse folding." Since the pulsar period is assumed to be known, a time series representing some relevant quantity, $X(t)$, can be written as $X_i(\phi)$, where ϕ refers to the pulse phase and i represents the pulse number. In the span of one pulsar period, ϕ varies from 0 to 1. Hence, $X_i(\phi)$ represents the quantity X at pulse phase ϕ of the ith pulse in the time series or, equivalently, at time $t = (\phi + i)\mathscr{P}$, where $\mathscr{P}$ is the pulsar period. The pulse-ensemble average of some function of this quantity, $f(X)$, is defined as

$$\langle f(\phi)\rangle \approx \frac{1}{N}\sum_{i=0}^{N-1} f(X_i(\phi)) , \tag{1}$$

where N is the total number of pulses in the data set.

3.2. *Autocorrelation Functions*

Given two measured quantities, $X_i(\phi)$ and $Y_i(\phi)$, the cross-correlation function of these quantities computed within a pulse phase region starting at ϕ_0 and ending at ϕ_1 for the ith pulse is defined as

$$C^i_{XY}(\Delta\phi) \equiv \frac{1}{\phi_1 - \phi_0}\int_{\phi_0}^{\phi_1} X_i(\phi) Y_i(\phi + \Delta\phi)\, d\phi . \tag{2}$$

If $Y_i = X_i^*$, then the above equation defines the autocorrelation function (ACF), and is denoted as $C^i_X(\Delta\phi)$. For the case of discretely sampled data, the above integral becomes a sum of the discrete points. Note that cyclic boundary conditions are assumed when evaluating the above expression for the case when $\phi + \Delta\phi$ lies outside the interval $[\phi_0, \phi_1]$.

The recorded voltage signal contains two components: a signal component and a noise component. Since only the correlation functions of the signal are of interest, the contribution of the noise terms must be subtracted off. The recorded complex voltage signal, $V(t)$, can be expressed as

$$V(t) = S(t) + N(t) , \tag{3}$$

where $S(t)$ is the pulsar signal, and $N(t)$ is the system noise plus the sky background noise. The signal intensities are defined as follows:

$$I_v(t) = V(t)^* V(t) , \tag{4}$$

$$I_s(t) = S(t)^* S(t) , \tag{5}$$

$$I_n(t) = N(t)^* N(t) . \tag{6}$$

Using the above definitions, the ensemble-averaged voltage autocorrelation function,

$$\langle C_V(\Delta\phi)\rangle \equiv \frac{1}{N}\sum_{i=0}^{N-1} C^i_V , \tag{7}$$

can be written as

$$\langle C_V(\Delta\phi)\rangle = \langle C_S(\Delta\phi)\rangle + \langle C_N(\Delta\phi)\rangle , \tag{8}$$

and the ensemble-averaged intensity autocorrelation function, $\langle C_{I_v}(\Delta\phi)\rangle$, is expressed as

$$\begin{aligned}\langle C_{I_v}(\Delta\phi)\rangle = {} & \langle C_{I_s}(\Delta\phi)\rangle + \langle C_{I_n}(\Delta\phi)\rangle \\ & + 2\langle I_s\rangle\langle I_n\rangle \\ & + 2\mathrm{Re}[\langle C_{S^*S^*}(\Delta\phi)\rangle\langle C_{NN}(\Delta\phi)\rangle] \\ & + 2\mathrm{Re}[\langle C_S(\Delta\phi)\rangle\langle C_N(\Delta\phi)\rangle] ,\end{aligned} \tag{9}$$

where $\langle I_s\rangle$ and $\langle I_n\rangle$ are the average signal intensity and noise intensity, respectively, within the pulse phase window, and, consequently, are independent of $\Delta\phi$. The above relationships were calculated assuming that the noise and the signal are statistically independent. Using a phase region where $S(\phi) = 0$, all of the noise correlation functions can be estimated, and the above relationships can be used to calculate the autocorrelation functions of the signal alone:

$$\langle C_S(\Delta\phi)\rangle = \langle C_V(\Delta\phi)\rangle - \langle C_N(\Delta\phi)\rangle , \tag{10}$$

$$\begin{aligned}\langle C_{I_s}(\Delta\phi)\rangle = {} & \langle C_{I_v}(\Delta\phi)\rangle - C_{I_n}(\Delta\phi) - 2\langle I_s\rangle\langle I_n\rangle \\ & - 2\mathrm{Re}[(\langle C_{V^*V^*}(\Delta\phi)\rangle - \langle C_{N^*N^*}(\Delta\phi)\rangle)\langle C_{NN}(\Delta\phi)\rangle] \\ & - 2\mathrm{Re}[(\langle C_V(\Delta\phi)\rangle - \langle C_N(\Delta\phi)\rangle)\langle C_N(\Delta\phi)\rangle] .\end{aligned} \tag{11}$$

3.3. *The Modified Coherence Function*

The main goal of this work is to establish the existence of coherent non-Gaussian statistics in the received radiation field. One way to search for this is to calculate the "modified coherence function" (MCF),

$$M_s(\Delta\phi) \equiv \frac{\langle C_{I_s}(\Delta\phi)\rangle}{\langle C_{I_s}(0)\rangle} - \frac{1}{2}\left[\left|\frac{\langle C_S(\Delta\phi)\rangle}{\langle C_S(0)\rangle}\right|^2 + 1\right], \tag{12}$$

where the vertical bars, $|\ldots|$, represent the complex absolute value. For stationary Gaussian statistics, the intensity

autocorrelation function takes the form

$$\langle C_{I_s}(\Delta\phi)\rangle = \langle I_s\rangle^2 + |\langle C_S(\Delta\phi)\rangle|^2 . \quad (13)$$

Substituting the above relationship into equation (12) shows that $M_s(\Delta\phi) = 0$ for stationary Gaussian statistics. Note that $C_S(0) = \langle I_s\rangle$. For the case of amplitude-modulated Gaussian noise, the signal can be expressed as

$$S(t) = G_n(t)A(t) , \quad (14)$$

where G_n is a stationary Gaussian signal, and A is a slowly varying amplitude function. The MCF of an amplitude-modulated Gaussian-noise process takes the form

$$M_s(\Delta\phi) = \frac{1}{2}\left[\left|\frac{\langle C_{G_n}(\Delta\phi)\rangle}{\langle C_{G_n}(0)\rangle}\right|^2 - 1\right] \times \left[\frac{\langle C_{|A|^2}(\Delta\phi)\rangle}{\langle C_{|A|^2}(0)\rangle} - \left|\frac{\langle C_A(\Delta\phi)\rangle}{\langle C_A(0)\rangle}\right|^2\right] + M_A , \quad (15)$$

where M_A is the MCF of the amplitude function. If A also obeys Gaussian statistics, then the MCF becomes

$$M_s(\Delta\phi) = \frac{1}{4}\left[\left|\frac{\langle C_{G_n}(\Delta\phi)\rangle}{\langle C_{G_n}(0)\rangle}\right|^2 - 1\right]\left[1 - \left|\frac{\langle C_A(\Delta\phi)\rangle}{\langle C_A(0)\rangle}\right|^2\right] . \quad (16)$$

The above expression is never greater than zero. Hence, a clear signature of non-Gaussian statistics occurs when $M_s(\Delta\phi) > 0$. The coherence time, τ_c, is defined as that value of $\Delta\phi$ where $M_s(\Delta\phi)$ crosses zero.

Since Gaussian statistics remain Gaussian statistics under any type of linear transformation, amplitude-modulated Gaussian noise will remain amplitude-modulated Gaussian noise regardless of any linear interstellar medium (ISM) propagation effects and any linear signal processing. Note that ISM scattering is a linear propagation effect. Since dedispersion is a linear process as well, a slight error in the dispersion measure will not affect the fact that the statistics are Gaussian. Therefore, propagation effects, filter response effects, and incorrect DM effects would not cause $M_s(\Delta\phi) > 0$ if the statistics were initially Gaussian. These effects may turn non-Gaussian noise into Gaussian noise, and they may alter the coherence time of a non-Gaussian signal. Such effects must be well understood in order to correctly interpret a non-Gaussian signature, but they need not be well understood in order to detect a non-Gaussian signature.

The process of digitization is a nonlinear process, and it will introduce artifacts into $M_s(\Delta\phi)$. Fortunately, these artifacts are severely reduced when the digitized time series is coherently dedispersed. With dispersion measures greater than 1 pc cm^{-3} at a center frequency of 430 MHz, the dedispersion filter spreads these artifacts over a timescale that is much larger than any considered here. Analysis of simulated data has confirmed this statement. Unfortunately, this is not necessarily the case for observations at a center frequency of 1 GHz and above. Hence, for the 430 MHz observations presented in this paper, the digitization effects can be ignored.

In order to remove effects that are associated with gain- and noise-level variations that occur as the Arecibo telescope tracks the source, the MCF was calculated every 107 seconds, and the resulting MCFs were averaged together. Such variations will only affect the MCF if the signal is non-Gaussian.

4. ANALYSIS RESULTS

Modified coherence functions have been calculated using data from four pulsars: B1937+21, B0823+26, B0950+08, and B1133+16 (see Fig. 1). For each object, the ensemble-averaged autocorrelation functions were calculated using

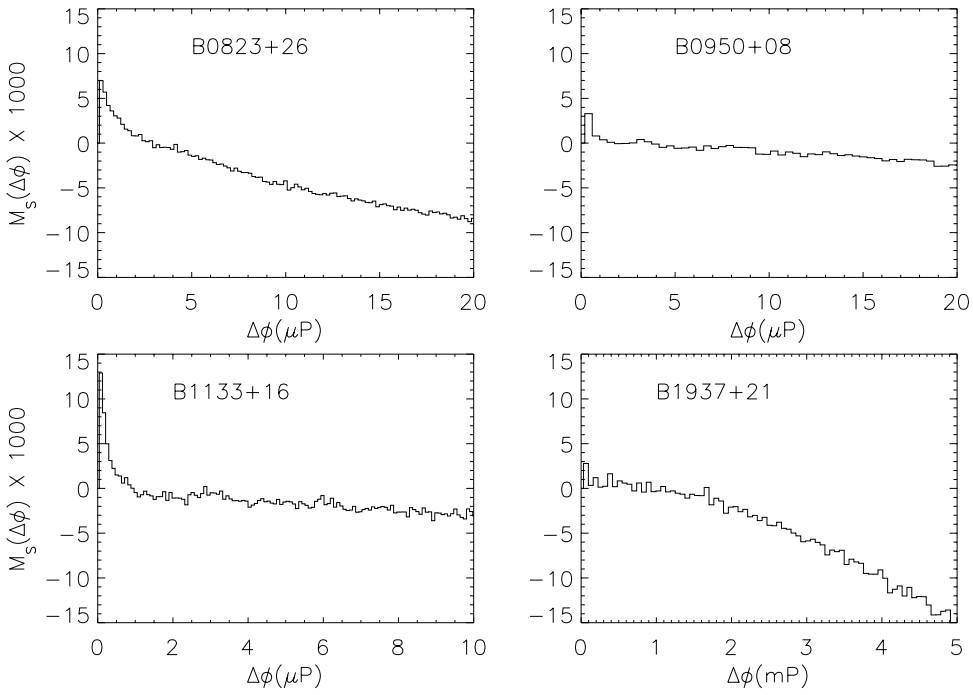

FIG. 1.—Modified coherence functions measured for pulsars B0823+26, B0950+08, B1133+16, and B1937+21. The time resolution for each MCF is 100 ns. Both polarizations were analyzed separately, and the resulting MCFs were averaged together to increase the signal-to-noise ratio.

TABLE 2

ANALYSIS PARAMETERS

Parameter	B0823+26	B0950+08	B1133+16	B1937+21
N	12300	15700	3240	2.74×10^6
ϕ_0 (m$\mathscr{P}$).....	−2.650	−9.844	−0.016	−93
ϕ_1 (m$\mathscr{P}$).....	−1.106	−8.225	0.674	170
N_t.....	8192	4096	8192	4096

N_t time samples in a region of pulse phase starting at ϕ_0 and ending at ϕ_1. The ensemble consisted of N pulses. The values of N, N_t, ϕ_0, and ϕ_1 are given in Table 2. Each circular polarization component was analyzed separately, and the resulting MCFs were averaged together to increase the signal-to-noise ratio. The astrometric and spin parameters for these objects are given in Table 1. For reference purposes, the average pulse profiles are given in Figure 2. In each case, the phase origin is taken to be the location of the peak average intensity.

5. CONSTRAINTS ON THE EMISSION MECHANISM

The signature of coherent non-Gaussian statistics is clearly observed in pulsars B0823+26, B0950+08, and B1133+16. As previously discussed, $M_s(\Delta\phi)$ could only be greater than zero if the intrinsic signal had non-Gaussian statistics. If the intrinsic signal had Gaussian statistics, linear filtering effects associated with ISM propagation and signal processing would not cause the modified coherence function to be significantly greater than zero. These effects would alter a non-Gaussian signal. The coherence time and the amplitude of the observed features could be affected.

In this work, the above results are compared with a shot noise model. This type of model was originally proposed by Cordes (1976). The amplitude and timescales of the observed features in the MCF can be related to the rate and lifetime of randomly distributed coherent shots. In the absence of propagation and signal-processing effects, these numbers would describe the fundamental emitters responsible for the radio emission.

5.1. *Generalized Complex Shot Model*

Let S be a complex time series defined on a phase region of length T that consists of a sum of individual complex "shots",

$$S(\phi) = \sum_{i=0}^{N-1} f(\hat{v}_i, \phi - \phi_i) , \tag{17}$$

where N is the total number of shots that occurred in the interval of length T, $f(\hat{v}, \phi)$ is a parameterized function of pulse phase or, equivalently, time that describes each individual shot, $\hat{v}_i$ is a vector of parameters that characterize the ith shot, and ϕ_i is the arrival time of the ith shot. Since this is a model for the received field within a pulse phase region, the temporal parameter will be represented by ϕ. Note that $\Delta\phi = \Delta t/\mathscr{P}$, where $\mathscr{P}$ is the pulsar period. Next, let $P(\hat{v}_i, \phi_i)$ be the probability density function for a shot occurring within $[\phi_i, \phi_i + d\phi_i]$, with parameters between $[\hat{v}_i, \hat{v}_i + d\hat{v}_i]$.

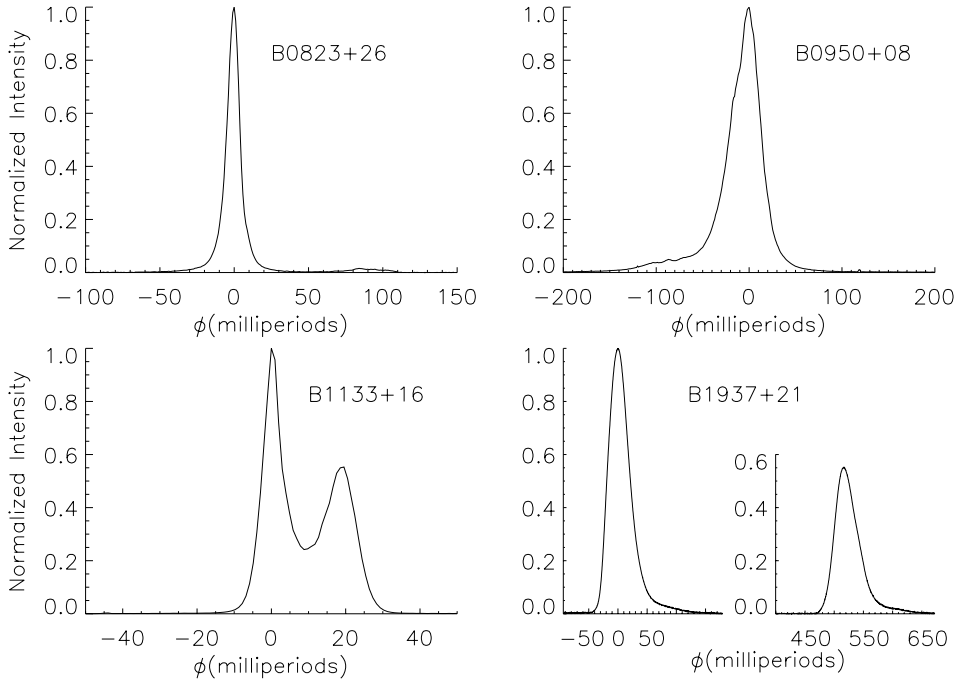

FIG. 2.—Average pulse profiles of pulsars B0823+26, B0950+08, B1133+16, and B1937+21, with time resolutions of 0.52, 0.25, 1.2 ms, and 0.42 μs, respectively. B1937+21 was calculated after the data were coherently dedispersed, while the other three profiles were calculated after the data were incoherently dedispersed. Pulsars B0823+26 and B0950+08 were analyzed with 512 filter-bank channels and 1024 phase bins. Pulsar B1133+16 was analyzed with 1024 filter-bank channels and 1024 phase bins.

The ensemble-averaged value of $S(\phi)$ is given by

$$\langle S(\phi)\rangle = N\langle f(\hat{v}_i,\ \phi - \phi_i)\rangle\ , \tag{18}$$

$$= N\int P(\hat{v}_i,\ \phi_i) f(\hat{v}_i,\ \phi - \phi_i)\, d^n v_i\, d\phi_i\ . \tag{19}$$

A few simplifying assumptions will now be made. First, $\langle S\rangle = 0$. Second, the shot arrival times are uniformly distributed over the total time interval T. Third, the statistics of the shots are independent from one another. Hence, $P(\hat{v}_i,\ \phi_i) = P(\hat{v}_i)/T$, and the joint probability function, $P(\hat{v}_i,\ \hat{v}_j,\ \phi_i,\ \phi_j)$, is given by $P(\hat{v}_i,\ \phi_i)P(\hat{v}_j,\ \phi_j)$. With the above definitions and assumptions, the ensemble-averaged autocorrelation functions, $\langle C_S\rangle$ and $\langle C_{I_s}\rangle$, can be expressed as

$$\langle C_S(\Delta\phi)\rangle = \frac{N}{T}\int P(\hat{v}_i) f^*(\hat{v}_i,\ \phi_i) \times f(\hat{v}_i,\ \phi_i + \Delta\phi)\, d^n v_i\, d\phi_i\ , \tag{20}$$

$$\langle C_{I_s}(\Delta\phi)\rangle = \frac{N}{T}\int P(\hat{v}_i)\,|f(\hat{v}_i,\ \phi_i)|^2 \times |f(\hat{v}_i,\ \phi_i + \Delta\phi)|^2\, d^n v_i\, d\phi_i + \left(1 - \frac{1}{N}\right)(|C_S(\Delta\phi)|^2 + |C_S(0)|^2)\ . \tag{21}$$

Next, we define the individual shot autocorrelation functions,

$$C_f(\hat{v}_i,\ \Delta\phi) \equiv \frac{1}{T}\int f^*(\hat{v}_i,\ \phi) f(\hat{v}_i,\ \phi + \Delta\phi)\, d\phi\ , \tag{22}$$

$$C_{I_f}(\hat{v}_i,\ \Delta\phi) \equiv \frac{1}{T}\int |f(\hat{v}_i,\ \phi)|^2\, |f(\hat{v}_i,\ \phi + \Delta\phi)|^2\, d\phi\ , \tag{23}$$

and their ensemble averages,

$$\langle C_f(\Delta\phi)\rangle = \int P(\hat{v}_i) C_f(\hat{v}_i,\ \Delta\phi)\, d^n v_i\ , \tag{24}$$

$$\langle C_{I_f}(\Delta\phi)\rangle = \int P(\hat{v}_i) C_{I_f}(\hat{v}_i,\ \Delta\phi)\, d^n v_i\ . \tag{25}$$

With the above definitions, equations (20) and (21) become

$$\langle C_S(\Delta\phi)\rangle = N\langle C_f(\Delta\phi)\rangle\ , \tag{26}$$

$$\langle C_{I_s}(\Delta\phi)\rangle = N\langle C_{I_f}(\Delta\phi)\rangle + (N^2 - N) \times (\langle |C_f(\Delta\phi)|^2\rangle + \langle |C_f(0)|^2\rangle)\ . \tag{27}$$

The modified coherence function for stationary shot noise can be found by substituting equations (26) and (27) into the definition of M_s (eq. [12]),

$$M_s(\Delta\phi) = \frac{1}{1 + 2R\tau_c(1 - 1/N)}\, M_f(\Delta\phi)\ , \tag{28}$$

$$M_f(\Delta\phi) \equiv \frac{\langle C_{I_f}(\Delta\phi)\rangle}{\langle C_{I_f}(0)\rangle} - \frac{1}{2}\left[\left|\frac{\langle C_f(\Delta\phi)\rangle}{\langle C_f(0)\rangle}\right|^2 + 1\right], \tag{29}$$

where $R = N/T$ and τ_c is a characteristic timescale defined as

$$\frac{\tau_c}{T} \equiv \frac{|\langle C_f(0)\rangle|^2}{\langle C_{I_f}(0)\rangle}\ . \tag{30}$$

This characteristic timescale is of the order of the average width of the individual shots. Heuristically, this can be seen by taking f to be a square wave of width W and amplitude 1. Both $\langle C_f(0)\rangle$ and $\langle C_{I_f}(0)\rangle$ are equal to W/T. Hence, $\tau_c = W$.

For the case of $N \gg 1$ and $R\tau_c \gg 1$, the modified coherence function takes on the following simplified form,

$$M_s(\Delta\phi) = \frac{1}{2R\tau_c}\, M_f(\Delta\phi)\ . \tag{31}$$

5.2. *Three Specific Shot Models*

The modified coherence function, $M_s(\Delta\phi)$, for a specific shot noise model can be calculated using equations (29) and (31). In this section, M_s is calculated for three important examples.

5.2.1. *Amplitude-Modulated Gaussian Shots*

In this case, f is given by

$$f(v_0,\ v_1,\ \phi) = v_0\, a(\phi) n(\phi,\ v_1)\ , \tag{32}$$

where $n(\phi,\ v_1)$ is a delta-correlated noise process with a "random seed" v_1 and with $\langle |n|^2\rangle = 1$, $a(\phi)$ is an amplitude-modulating function with a maximum of 1 at $\phi = 0$, and v_0 is the amplitude of the shot. For purposes of simplicity, $a(\phi)$ is the same for all shots. This type of model has been used to describe pulsar subpulses and microstructure (Smirnova 1988; Bartel & Hankins 1982; Rickett 1975). The random seed parameter allows one to differentiate between the random noise process in two different shots. Assuming that the probability of v_1 is independent of all other quantities, the following relationships hold:

$$\int P(v_1) n^*(\phi,\ v_1) n(\phi + \Delta\phi,\ v_1)\, dv_1 = \delta(\Delta\phi)\ , \tag{33}$$

$$\int P(v_1)\,|n(\phi,\ v_1)|^2\, |n(\phi + \Delta\phi,\ v_1)|^2\, dv_1 = 1 + \delta(\Delta\phi)\ . \tag{34}$$

For discrete data, $\delta(\Delta\phi)$ is the Kronecker delta function. The modified coherence function for this model is given by

$$M_s(\Delta\phi) = \frac{1}{4R\tau_c}\left[\frac{C_{|a|^2}(\Delta\phi)}{C_{|a|^2}(0)} - 1\right]. \tag{35}$$

Hence, for amplitude-modulated Gaussian shots, M_s is zero for $\Delta\phi \ll \tau_c$, and goes to $-(4R\tau_c)^{-1}$ for $\Delta\phi \gg \tau_c$. In general, when the shot model is based on stationary or nonstationary amplitude-modulated Gaussian noise, $M_s(\Delta\phi) \leq 0$.

5.2.2. *Coherent Square Wave Shots*

For this model, f is given by

$$f(v_0,\ \phi) = v_0\, \mathrm{sq}(\phi)\ , \tag{36}$$

where $\mathrm{sq}(\phi)$ is a square wave of amplitude 1 and width W, and $\langle v_0\rangle = 0$. Equations (22)–(25) show that $\langle C_f(\Delta\phi)\rangle/\langle C_f(0)\rangle = \langle C_{I_f}(\Delta\phi)\rangle/\langle C_{I_f}(0)\rangle$, with

$$\frac{\langle C_f(\Delta\phi)\rangle}{\langle C_f(0)\rangle} = \begin{cases} 1 - \Delta\phi/W & \text{if } \Delta\phi \leq W, \\ 0 & \text{if } \Delta\phi > W. \end{cases} \tag{37}$$

Hence, the MCF becomes

$$M_s(\Delta\phi) = \frac{1}{2R\tau_c}\begin{cases} -\frac{1}{2}(\Delta\phi/W)^2 & \text{if } \Delta\phi \leq W, \\ -\frac{1}{2} & \text{if } \Delta\phi > W. \end{cases} \tag{38}$$

This model generates a modified coherence function that looks similar to the MCF generated by the amplitude-modulated Gaussian-noise model. Here, M_s starts at zero and decreases to $-(4R\tau_c)^{-1}$ as $\Delta\phi$ increases. Hence, the MCF cannot be used to distinguish between simple coherent shot models, such as the one presented above, and amplitude-modulated Gaussian-noise models.

5.2.3. *Narrowband Shots*

Consider the set of functions given by

$$f(A, \omega, \psi_0, \phi) = A \exp(i\omega\phi + \psi_0)a(\phi) , \quad (39)$$

where A, ω, and ψ_0 are the shot parameters, which correspond to amplitude, frequency, and initial phase, respectively. The function $a(\phi)$ is an amplitude-modulating function with a maximum at $a(0) = 1$. This model describes narrowband shots, each with a different frequency. Assuming that each parameter is statistically independent, and that ω and ψ_0 are uniformly distributed, the MCF for this model is given by

$$M_s(\Delta\phi) = \frac{1}{2R\tau_c}\begin{cases}[\langle C_{|a|^2}(\Delta\phi)\rangle/\langle C_{|a|^2}(0)\rangle] - \frac{1}{2} & \text{if } \Delta\phi > 0, \\ 0 & \text{if } \Delta\phi = 0.\end{cases} \quad (40)$$

In this model, M_s is greater than zero for small $\Delta\phi$, except when $\Delta\phi = 0$. The peak height is of order $(4R\tau_c)^{-1}$.

5.3. *Comparison with the Data*

The properties of Gaussian statistics ensure that $M_s \leq 0$ for any model based on amplitude-modulated Gaussian noise with an amplitude-modulating function obeying Gaussian statistics. Hence, such a model is ruled out. Amplitude-modulated Gaussian-noise models with $M_A > 0$ will cause $M_s > 0$, but direct calculations have shown that $M_A < 0$ for several types of positive-definite amplitude functions, including square wave, Gaussian, and squared sinusoidal functions. Simple computer experiments that randomly generate positive-definite functions and then calculate the MCF have shown that the MCF is less then zero. Hence, it is highly likely that $M_A < 0$ for admissible amplitude-modulating functions. Of the three shot models described above, only the narrowband shot model generates an MCF with M_s greater than zero for small values of $\Delta\phi$. It is highly possible that digitization effects, along with coherently dedispersing the data with an incorrect dispersion measure, will alter M_s in such a way that the second model (the coherent square wave model) may have an MCF that behaves like M_s for the narrowband shot model. Composite models made up of shots from the first and second model described above can be shown to have $M_s > 0$. Therefore, until a better understanding of various possible models, propagation effects, and processing artifacts is obtained, no further conclusions can be drawn concerning the validity of the various models or the structure of the individual shots. Regardless, the modified coherence function can provide an estimate of $R\tau_c$, where R is the shot rate (i.e., the number of shots occurring per unit time), and τ_c is the characteristic temporal width of each shot, assuming that the shot model is correct. The product, $R\tau_c$, is the average number of shots that occur within the width of a single shot. Assuming that $M_f(\Delta\phi)$ is of order unity for small nonzero values of $\Delta\phi$, equation (31) shows that $M_s(\Delta\phi)$ is of the order of $(R\tau_c)^{-1}$. Using the measured value of M_s at a pulse phase lag corresponding to one time sample ($\delta t = 100$ ns), $R\tau_c$ can be estimated even though the exact details of the shot model are not known. One can also estimate the intensity of an individual shot from the relationship

$$\langle I_s\rangle = R\tau_c\langle I_{\rm shot}\rangle , \quad (41)$$

where $\langle I_s\rangle$ is the average signal intensity, and $\langle I_{\rm shot}\rangle$ is the average intensity of a single shot. Note that each polarization is considered separately in this analysis. The coherence time, τ_c, can be estimated using that value of $\Delta\phi$ where $M_s(\Delta\phi) = 0$. Table 3 lists the measured values of $R\tau_c$, τ_c, and $\langle I_{\rm shot}\rangle$ for each pulsar observed. For the case of B1937+21, appropriate limits are placed on these quantities based on the noise level present in M_s. Note that the values of $\langle I_s\rangle$ were estimated from peak flux values calculated using previously published data from Taylor, Manchester, & Lyne (1993). Ignoring all propagation effects, except for the D^{-2} scaling of the intensity, one can estimate the average specific intensity of a fundamental emission event occurring near the pulsar,

$$\frac{dP_e}{dvd\Omega} = \frac{D^2\langle I_s\rangle}{R\tau_c} , \quad (42)$$

$$= \frac{D_{\rm kpc}^2 S_{\rm mJy}}{R\tau_c} 10^{17}\text{ergs s}^{-1}\text{ Hz}^{-1} , \quad (43)$$

where $D_{\rm kpc}$ is the distance to the pulsar in kiloparsecs, $S_{\rm mJy}$ is the average power flux in milliJanskys, and $dP_e/dv/d\Omega$ is the average power per unit frequency per unit solid angle per fundamental emitter. Furthermore, if the narrowband shot model is adopted, the measured coherence time can be used to estimate the quantity $\Delta f/f$, where Δf is the spectral width of the narrowband emission, and f is the center frequency of the emission event. This model corresponds to a class of "maser-type" emission mechanisms. The term $\Delta f/f$

TABLE 3

MEASURED SHOT PARAMETERS

Parameter	B0823+26	B0950+08	B1133+16	B1937+21
$R\tau_c$	143	304	77	>1200
τ_c (μP)	2.82	1.58	0.926	...
τ_c (μs)	1.5	0.4	1.1	...
Peak flux (Jy)	5	10	13	4
$\langle I_{\rm shot}\rangle$ (mJy)	35	33	169	<3
$dP_e/dv/d\Omega$ (10^{17} ergs s^{-1} Hz^{-1})	5	0.6	12	<42
$\Delta f/f$ (10^{-3})	1.6	5.8	2.1	...

can be estimated using the relationship

$$\frac{\Delta f}{f} \approx \frac{1}{\tau_c f}, \tag{44}$$

where f is taken to be 430 MHz, the center frequency of the observations. The calculated values for $\Delta f/f$ and $dP_e/dv/d\Omega$ are also listed on Table 3. Note that until the effects of ISM propagation and digital signal processing on non-Gaussian signals are better understood, all values listed on Table 3 should be taken as order-of-magnitude estimates at best. Since the ISM tends to increase the coherence time, τ_c is an upper bound of the actual coherence time.

6. SUMMARY AND CONCLUSIONS

Using the modified coherence function (MCF) defined in § 3.3, coherent non-Gaussian emission has been detected in three of the four pulsars observed in this study (B0823+26, B0950+08, and B1133+16). For a Gaussian noise signal, the MCF is always less than or equal to zero regardless of any linear filtering performed on the data set. This rules out possible artifacts generated by ISM propagation effects, as well as effects due to dedispersing with a slightly incorrect value of the dispersion measure. Digitization effects may create artifacts in the MCF, but simulations have shown that these effects are negligible when the dedispersion filter response time is much larger than any timescale of interest.

The observed MCFs have been interpreted in the framework of a coherent shot noise model. Even though the exact details of the shots cannot be determined from the data until ISM propagation and signal-processing effects are better understood, various important physical quantities can still be estimated. Of particular importance is the shot rate multiplied by its temporal width, $R\tau_c$, and the power flux per shot. These quantities are estimated from the data to be of the order of 100 and 100 mJy, respectively. Ignoring propagation effects that may alter both of these observed quantities, the specific intensity of a single fundamental emission event is given by the square of the distance to the pulsar times the ratio of the local observed shot intensity to $R\tau_c$. This has been estimated from the data to be of the order of 10^{17} ergs s^{-1} Hz^{-1}. The coherence time of the emission events is approximately given by the time lag where M_s equals zero. These times have been estimated to be of the order of 1 μs. Note that ISM propagation effects would tend to increase the coherence time; hence, the measured value is an upper bound on the actual coherence time.

These results do not rule out the possibility that the emission is an amplitude-modulated Gaussian-noise process with an amplitude function satisfying $M_A > 0$, since $M_s < 0$ if and only if $M_A < 0$ in the case of a general amplitude-modulating function. It can be shown that $M_A < 0$ for square-wave, Gaussian, and one-sided exponential amplitude functions. Simple computer "experiments" have shown that $M_A < 0$ for randomly generated, slowly varying positive-definite functions. Hence, it is possible that $M_A < 0$ for amplitude functions that are allowable in the amplitude-modulated Gaussian-noise model.

The detection of coherent non-Gaussian radio emission places an enormous constraint on the basic emission mechanism. Theoretical models now have to explain the shape of the MCF without relying on the central limit theorem to average away the coherent effects of the basic plasma radio-emission process. Currently, few models are detailed enough to provide a calculation of the expected MCF. In principal, pulsar radio-emission models based on coherent curvature emission (Buschauer & Benford 1976) and Langmuir solitons (Asseo, Pelletier, & Sol 1990; Weatherall 1998) are detailed enough to provide theoretical predictions for the MCF. Weatherall (1998) calculates $C_{I_f}(\Delta\phi)/C_{I_f}(0)$ for a model based on Langmuir soliton emission. Since C_f is nearly a delta function for this model, M_s is approximately given by $C_{I_f}(\Delta\phi)/C_{I_f}(0) - 1/2$. Unfortunately, the structure of the MCF predicted by Weatherall's model is not supported by the data. Asseo et al. (1990) also investigated a model based on Langmuir solitons. They estimated the maximum specific intensity of a fundamental emitter under typical pulsar plasma conditions to be of the order of 10^{21} ergs s^{-1} Hz^{-1}, well above the values measured in this paper. They also predict the number of emitters to be of order $10^3\mathcal{P}^{1/3}$ where $\mathcal{P}$ is the pulsar period in seconds. This relationship is also not supported by the data.

The observations and analysis presented here represent a very small subset of possible investigations that can be performed on the coherent radio signals. By observing a larger sample of pulsars, including both slow and millisecond pulsars, various relationships can be determined between the MCF shape, R, τ_c, $dP_e/dv/d\Omega$, and various fundamental pulsar parameters including period, period derivative, surface magnetic field strength, light cylinder radius, and magnetic inclination angle. The polarization properties and frequency structure of the individual shots need to be investigated along with the variation of the shot parameters as a function of pulse phase. Such analyses will further constrain the basic emission process and help illuminate the structure of pulsar magnetospheres.

The authors would like to acknowledge Caltech's Center for Advanced Computation and Research for the use of their facilities. We also thank Roger Blandford, Yoram Lithwick, Maxim Lyutikov, and Andrew Melatos for stimulating discussions. This work was supported in part by the National Science Foundation under NSF grants COA 9318145 and AST 98-19926.

REFERENCES

Asseo, E., Pelletier, G., & Sol, H. 1990, MNRAS, 247, 529
Bartel, N., & Hankins, T. H. 1982, ApJ, 254, L35
Buschauer, R., & Benford, G. 1976, MNRAS, 177, 109
Cordes, J. M. 1976, ApJ, 210, 780
Cordes, J. M., & Rickett, B. J. 1998, ApJ, 507, 846
Gil, J. 1985, Ap&SS, 110, 293
Hankins, T. H. 1996, in IAU Colloq. 160, Pulsars: Problems and Progress, ed. S. Johnston & M. A. Walker (San Francisco: ASP), 197
Hankins, T. H., & Rickett, B. J. 1975, Methods Comput. Phys., 14, 55
Jenet, F. A., & Anderson, S. B. 1998, PASP, 110, 1467
Jenet, F. A., Cook, W. R., Prince, T. A., & Unwin, S. C. 1997, PASP, 109, 707
Melrose, D. B. 1992, in IAU Colloq. 128, Magnetospheric Structure and Emission Mechanisms of Radio Pulsars, ed. T. H. Hankins, J. M. Rankin, & J. A. Gil (Zielona Gora: Pedagogical Univ. Press), 306
Rickett, B. J. 1975, ApJ, 197, 185
Rickett, B. J. 1998, BAAS, 192, 4601
Smirnova, T. V. 1988, Soviet Astron. Lett., 14, 20
Stineberg, D. R. 1982, Ph.D. thesis, Cornell Univ., Ithaca
Taylor, J. H., Manchester, R. N., & Lyne, A. G. 1993, ApJS, 88, 529
Taylor, J. H., & Weisberg, J. M. 1989, ApJ, 345, 434
Weatherall, J. C. 1998, ApJ, 506, 341